Preprints of the 21st IFAC World Congress (Virtual)
Berlin, Germany, July 12-17, 2020

Design of Fractional-Order Lag Network and Fractional-Order PI Controller for a Robotic Manipulator

Petar D. Mandić * **Paolo Lino** *** **Guido Maione** ***
Mihailo P. Lazarević * **Tomislav B. Šekara** **

* *Faculty of Mechanical Engineering, University of Belgrade, Kraljice Marije 16, Belgrade, Serbia (e-mail: pmandic@mas.bg.ac.rs, mlazarevic@mas.bg.ac.rs).*
** *School of Electrical Engineering, University of Belgrade, Bulevar kralja Aleksandra 73, Belgrade, Serbia (e-mail: tomi@etf.rs).*
*** *Department of Electrical and Information Engineering, Polytechnic University of Bari, Via E. Orabona 4, Bari, Italy (e-mail: paolo.lino@poliba.it, guido.maione@poliba.it).*

Abstract: Motion control of robotic manipulators is frequently realized by independent control of the DC motors actuating robot joints. Namely, nonlinearities, coupling between actuators and other complex dynamics are neglected if high gear ratios between the actuators and robot joints are considered. This paper proposes a fractional-order lag network or a fractional-order PI controller to control the position of the actuators shafts. The introduced fractional compensators are designed by using the symmetrical optimum principle and by parameters optimization or by frequency-domain loop shaping, respectively. Simulation results and frequency response show effectiveness and robustness of the approach.

Keywords: Fractional-order lag compensator, fractional-order PI controller, robust control, frequency response, robotic manipulators, robot control.

1. INTRODUCTION

Robotics is a large inter-disciplinary field that is continuously growing and finding new applications. It requires knowledge of mechanical and electrical engineering, systems and control theory, and new technology. Research is stimulated by different applications and by the increasing demand in better performance of robotic systems. For example, robotic manipulators are spread in industry but present many issues in motion control because their dynamics is highly nonlinear, time-varying, and often subject to parametric uncertainty. To achieve a better compromise between performance and robustness, fractional-order control can provide a strategic hand to solve complex issues.

Industrial manipulators in automated factories must execute tasks with high accuracy and repeatability, and should be deployed to allow mass production and quality of products [5]. Although control is complex, manipulators can be controlled in a linear way if their dynamic model is assumed linear because of high gear ratios, gravity compensation devices, etc., or is linearized by feedback [26]. Then, nonlinear phenomena as well as dynamic coupling effects from the motion of other joints are neglected. In this way, the robot control problem can be decoupled into independent joint control. So, PID controllers are usually employed for the stabilization of manipulators [17].

In the last decades, application of fractional calculus to control problems has demonstrated several benefits [20; 22; 23; 25; 19]. Namely, fractional-order controllers have at disposal the fractional orders of integration and/or differentiation that can be used as additional degrees of freedom in controller design. In this way, not only performance can be increased, but especially robustness of the control loop is improved. To this aim, the seminal Bode's idea of the ideal open-loop gain based on a non-integer order integrator is fundamental [1]. Moreover, the compact structure of the controller is based on few parameters (tuning knobs) that allow to achieve similar or better results than integer-order controllers of high order. Literature shows successful applications to robot control [24; 18; 7; 29]. For example, robust path planning in 3-D space is achieved despite UAV mass variations [18]. In details, fractional attractive forces were introduced based on velocity fractional derivative.

In this paper, two types of fractional-order controllers of a robot manipulator are compared. A fractional-order lag network (FOLaN) is designed to achieve reference step response with no overshoot and iso-damping property, such that it is robust to large process gain variations. This property is very important in position control. Since FOLaN cannot reject disturbances completely, a fractional-order PI (FOPI) controller is designed with that purpose. It makes a compromise between performance and robustness, i.e. it is more sensitive to process gain variations, but disturbance is rejected with zero steady-state error. The two controllers are chosen because they are comparable and give similar results for the same design specifications,

Copyright lies with the authors

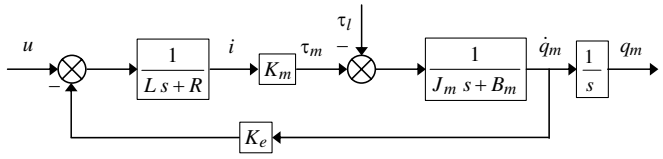

Fig. 1. Block scheme of the DC motor.

as shown by simulation, and require a lower design complexity than a fractional-order PID (FOPID) controller.

The paper is organized as follows. Section 2 describes the considered manipulator and derives its mathematical model. Section 3 explains how the introduced FOLaN and FOPI controllers are optimized and designed. Section 4 gives simulation results based on a linear dynamic model of a real manipulator. Section 5 gives some conclusions.

2. THE ROBOTIC MANIPULATOR

The robot manipulator consists of a sequence of mechanical rigid bodies (links) that are connected by joints. Here, the Rodriquez approach is used to obtain the equations of motion. The reader is referred to [6] for details regarding the mechanical model representing a chain of rigid bodies. If the kinetic energy is expressed in terms of generalized coordinates and their derivatives, then the system dynamic equations are written in terms of Lagrange equations of the second kind. The motion imposed to a joint is realized by an actuating system, which usually consists of a DC motor and a transmission (gear). After some transformations, the equations of motion of a rigid robot together with an actuating system can be written as:

$$[A(\mathbf{q}) + N^2\, J_m]\,\ddot{\mathbf{q}} + [C(\mathbf{q},\dot{\mathbf{q}}) + N^2\, B_m]\,\dot{\mathbf{q}} - \mathbf{Q}^g = \mathbf{Q}^m\,, \quad (1)$$

where, given the number n of bodies in the system, $\mathbf{q}(t) \in \mathbb{R}^n$ is the vector of the generalized coordinates, $A(\mathbf{q}) \in \mathbb{R}^{n\times n}$ is the basic metric tensor (inertia matrix), $C(\mathbf{q},\dot{\mathbf{q}}) \in \mathbb{R}^{n\times n}$ includes centrifugal and Coriolis effects, $\mathbf{Q}^g \in \mathbb{R}^n$ and $\mathbf{Q}^m \in \mathbb{R}^n$ are the gravity and torque terms applied to the joints, N is a $n \times n$ diagonal matrix of gear ratios, J_m is a $n\times n$ diagonal matrix of motor inertias, and, finally, B_m is a $n \times n$ diagonal matrix of viscous friction coefficients of the motors. Matrices $A(\mathbf{q})$ and $C(\mathbf{q},\dot{\mathbf{q}})$ are calculated as shown in [6]. The torques Q^m are supplied by n actuators. For a rigid robot, the equations describing the transmission of the gears are:

$$\mathbf{q}_m = N\,\mathbf{q} \;\text{ and }\; \mathbf{Q}^m = N\,\tau_i\,, \quad (2)$$

where $\mathbf{q}_m$ represents the positions of the actuators shafts and $\tau_i = (N^2)^{-1}\,[A(\mathbf{q})\,\ddot{\mathbf{q}}_m + C(\mathbf{q},\dot{\mathbf{q}})\,\dot{\mathbf{q}}_m] - N^{-1}\,\mathbf{Q}^g$ is the vector of torques resulting from the robot manipulator and acting on the motors shafts. Combination of (1) with (2) yields the following model of the actuators system

$$J_m\,\ddot{\mathbf{q}}_m + B_m\,\dot{\mathbf{q}}_m = \tau_m - \tau_i\,, \quad (3)$$

where τ_m is the vector of torques supplied by the actuators. Figure 1 shows a block scheme that represents the mechanical part of the DC motors by the model in (3). The positions of the actuators shafts are the controlled variables.

Two main advantages of the proposed approach are linearity and decoupling of the actuators model, which will be used for the controller design. Another key advantage is that the torque τ_l resulting from the robot links can be considered as a disturbance. This assumption is justified if actuators with high gear ratios are used, namely N typically takes on values from a few tens to a few hundreds. Then the robot nonlinear dynamics can be neglected.

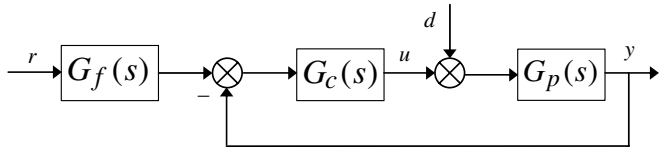

Fig. 2. The control scheme.

Finally, since the robot is commanded by voltage signals, a more realistic model must include the electrical part of the actuators as shown in Figure 1. Namely, the electrical model of the DC motor is given by

$$R\,i + L\,\frac{di}{dt} + K_e\,\frac{d\mathbf{q}_m}{dt} = \mathbf{u}\,, \quad (4)$$

where R is the $n \times n$ diagonal matrix containing the resistances of the armature circuits, $i \in \mathbb{R}^n$ is the vector of the armature currents, L is the diagonal matrix of the armature inductances, K_e is the diagonal matrix containing the back EMF constants, and $\mathbf{u}$ is the vector of the armature input voltages. The vector of torques supplied by the actuators is

$$\tau_m = K_m\,\mathbf{i}\,, \quad (5)$$

where K_m is the diagonal matrix of the torque constants.

To conclude the model, note that the robotic nonlinear system results into n linear, decoupled subsystems. Then, it is sufficient to analyze one arbitrary actuator (joint), perform its controller design, and extend the results to the other joints. On this basis, by Figure 1, the transfer function between the control input u and the position output of the j-th actuator, for $j = 1, ..., n$, is given by

$$G_p(s) = \frac{k_m}{(l\,s + r)\,(j_m\,s + b_m) + k_m\,k_e}\,\frac{1}{s} \approx \frac{K}{s\,(1 + T\,s)}\,, \quad (6)$$

in which $k_m \in K_m$, $l \in L$, $r \in R$, $j_m \in J_m$, $b_m \in B_m$, $k_e \in K_e$, $b_m \approx 0$, $K = \frac{1}{k_e}$, $T = \frac{j_m\,r}{k_m\,k_e}$. The approximation by a first-order system plus an integrator is motivated by the fact that one of the two poles from $(l\,s + r)\,(j_m\,s + b_m) + k_m\,k_e = 0$ is dominant on the other one.

3. CONTROLLER DESIGN

The control scheme is illustrated in Fig. 2, where $G_p(s)$ is the plant model, $G_c(s)$ is the employed controller, and $G_f(s)$ is a filter used to reduce overshoot and improve response to reference $r(t)$. Moreover, rejection of disturbance $d(t)$ must be achieved. Measurement noise is neglected.

The design of the considered controllers is based on the plant model given by:

$$G_p(s) = \frac{K}{s\,(1 + T\,s)}, \quad (7)$$

where K is the dc-gain and T is the time constant of the plant model. Time delays could be also compensated [10; 4].

The FOLaN and FOPI controllers are comparable. The difference between them is that FOPI rejects disturbance

signals with zero error, while FOLaN is more robust to variations in the process gain. Which controller is going to be used in certain situations depends on what are the primary design requirements. Obviously, a FOPID with more parameters to tune would provide better results, but its design is more complex and is not the goal of this paper.

3.1 Synthesis of Fractional-Order Lag Network

Generally speaking, the system transient response and robustness can be improved with fractional-order lead/lag controllers because they have more flexibility than integer-order controllers. Fractional compensators are more convenient to shape the frequency response and adjust the phase and gain margins in a sufficiently wide range around the crossover frequency. Moreover, it is well known that the phase margin affects the relative stability and the transient response characteristics, while the speed of response is determined by the bandwidth of the system. So, one could reshape the bandwidth and response speed by changing the gain crossover frequency. One could provide an enhanced robustness to gain variations and an iso-damping of the step response by obtaining a nearly constant phase around the crossover, thus a nearly constant phase margin.

The FOLaN is commonly used to improve tracking performance and disturbance attenuation at low frequencies. A lead network is used to improve phase margin and increase response speed. In this paper, a FOLaN is designed to enhance closed-loop performance of the robot manipulator.

The fractional-order lag network is specified by:

$$G_{c1}(s) = K_c \left(\frac{1 + a\,s}{1 + b\,s}\right)^{\alpha}, \tag{8}$$

where K_c is the dc gain, a and b are the zero and pole time constants thus determining the zero and pole locations ($-1/a$ and $-1/b$, respectively), with $a < b$ for a lag network, and $\alpha > 0$ is the fractional order.

Note that a proper choice of α is important because it affects the maximum delay and attenuation provided by the network. See [15] for similar arguments regarding a lead network. Namely, since

$$G_{c1}(j\omega) = K_c \left(\frac{1 + a\,j\omega}{1 + b\,j\omega}\right)^{\alpha}, \tag{9}$$

it is easy to find that

$$|G_{c1}(j\omega)| = K_c \left(\frac{1 + (a\,\omega)^2}{1 + (b\,\omega)^2}\right)^{0.5\,\alpha} \tag{10}$$

and, since $\angle G_{c1}(j\omega) = \alpha\,[\arctan(a\,\omega) - \arctan(b\,\omega)]$,

$$\angle G_{c1}(j\omega) = \alpha \arctan\left(\frac{\omega\,(a - b)}{1 + \omega^2\,a\,b}\right). \tag{11}$$

Phase and amplitude minimization are obtained at frequency $\omega_{min} = \frac{1}{\sqrt{a\,b}}$ such that

$$\varphi_{min} = \min \angle G_{c1}(j\omega) = \alpha \arctan\left(\frac{1 - \Delta}{2\sqrt{\Delta}}\right), \tag{12}$$

which is negative for all ω, and

$$M_{min} = \min |G_{c1}(j\omega)| = K_c\,\Delta^{-0.5\,\alpha}, \tag{13}$$

which is less than 1 for all ω, with $\Delta = \frac{b}{a} > 1$.

However, it is important to note that although α may change, the phase stays nearly constant around ω_{min}, which is remarkable to achieve robustness and the iso-damping property of the control system [23; 25; 19]. Note that the lower is α, the wider is the frequency range in which the phase of the compensated system is flat.

Most of the methods for tuning linear controllers are based on solving specific optimization problems that consider the main four sensitivity functions [27]. Other alternative methods such as the symmetrical optimum method have been developed [8] and successively adapted to fractional-order controllers design [16]. The main characteristic of this method is to make the Bode diagram of the open-loop frequency response $G(j\omega)$, then the phase margin behaviour $PM(\omega) = \angle G(j\omega) + \pi = \varphi(\omega) + \pi$, symmetrical with respect to the gain crossover frequency ω_{gc}.

Herein the FOLaN will be designed by using the principle of the symmetrical optimum method, which may be stated by specifying that several odd-order derivatives of the phase characteristic of $G(j\omega)$ should tend to zero in ω_{gc}:

$$\mu_p = \frac{\partial^p \varphi(\omega)}{\partial \omega^p}|_{\omega=\omega_{gc}} = 0 \quad p = 1, 3, 5, ... \tag{14}$$

Here only $p = 1, 3$ will be considered because (14) cannot hold for all values of p. However, a sufficient degree of symmetry around ω_{gc} will be achieved.

Another constraint is to achieve a desired phase margin PM_s in a specified ω_{gc}:

$$PM_s = \angle G(j\omega_{gc}) + \pi \text{ with } |G(j\omega_{gc})| = 1\,. \tag{15}$$

Then, the parameters K_c, a, b, and α of the FOLaN are obtained by solving an optimization problem [28; 2]:

$$\min(\mu_3)^2 \tag{16}$$

subject to

$$|G(j\omega_{gc})| = 1 \tag{17}$$

$$PM_s = \angle G(j\omega_{gc}) + \pi \tag{18}$$

$$\mu_1(K_c, a, b, \alpha) = 0 \tag{19}$$

To this aim, some standard nonlinear optimization methods are used by empirically selecting initial parameter values.

3.2 Synthesis of Fractional-Order PI controller

The fractional-order PI controller is defined by:

$$G_{c2}(s) = K_{p2} + \frac{K_{i2}}{s^{\nu}} = \frac{K_{p2}\,(1 + T_{i2}\,s^{\nu})}{T_{i2}\,s^{\nu}}, \tag{20}$$

with $T_{i2} = \frac{K_{p2}}{K_{i2}}$. Then the open-loop transfer function is:

$$G_2(s) = G_{c2}(s)\,G_p(s) = \frac{K_{i2}\,K\,(1 + T_{i2}\,s^{\nu})}{s^{1+\nu}\,(1 + T\,s)}. \tag{21}$$

It can be designed by an efficient procedure [9; 10] that shapes the open-loop frequency response

$$G_2(j\omega) = \frac{K_{i2}\,K\,[1 + T_{i2}\,\omega^{\nu}\,(C + jS)]}{\omega^{1+\nu}\,(-S + jC)\,(1 + j\,\omega\,T)} \tag{22}$$

around the gain crossover frequency ω_{gc}, where $C = \cos(0.5\,\pi\,\nu)$ and $S = \sin(0.5\,\pi\,\nu)$. The response $G_2(j\omega_{gc})$ is manipulated to obtain a desired constant phase margin

$$PM_s = \frac{\pi}{2}\,(1 - \nu), \tag{23}$$

which is strictly associated to the choice of ν. By (23), $\nu < 1$ should hold to obtain $0 < PM < \pi/2$. Moreover,

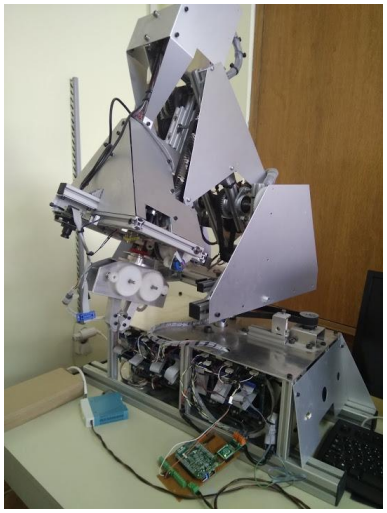

Fig. 3. The robotic manipulator.

(23) is obtained by adding π to the phase $\angle G_2(j\omega_{gc})$ and equating to zero the phase arguments that add to $\frac{\pi}{2}(1-\nu)$ and depend on T_{i2}, ω_{gc} and ν. This computation provides:

$$T_{i2} = \frac{\omega_{gc}\, T}{\omega_{gc}^{\nu}\,(S - \omega_{gc}\, T\, C)}\,, \tag{24}$$

which is anyway positive ($T_{i2} > 0$), while imposing a unitary gain at the gain crossover frequency determines

$$K_{i2} = \frac{\omega_{gc}^{\nu+1}}{K}\sqrt{\frac{1+\omega_{gc}^2\, T^2}{1+2\, C\, \omega_{gc}^{\nu}\, T_{i2} + \omega_{gc}^{2\nu}\, T_{i2}}}\,. \tag{25}$$

4. SIMULATION ANALYSIS

The robotic manipulator (Fig. 3) has six degrees of freedom: three revolute joints are used for positioning the end-effector, other three joints form the spherical wrist orientating the end-effector. Finally, there is the gripper. Herein position control is examined, then the model is simplified to three degrees of freedom (the first three joints).

Actually, two types of DC-motors are used for controlling the robot. The bigger one (maxon RE36, 70 Watt), which characteristics are used in simulation, is for motion control of the first three robot links, one motor for each link. The smaller type of motor (maxon A-max 22, 5 Watt) controls the last three links. Based on the parameters $J_m = 65.2\ \mathrm{g\,cm^2}$, $R = 1.71\,\Omega$, $k_m = 44.5 \cdot 10^{-3}\ \mathrm{N\,m/A}$, $k_e = 1/215$ V/rpm, the three DC motors that actuate the first three robot links are modeled by

$$G_p(s) = \frac{22.5148}{s\,(1+0.0055\, s)}\,, \tag{26}$$

and three controllers are based on this same plant model. The mechanical coupling between each DC motor and the actuated joint is realized by a pair of spur gears. The gear reduction ratio for each of the first three links is 230. A high reduction ratio tends to linearize the system and neglect the nonlinear coupling terms in the dynamic model.

The proposed fractional controllers are tested and compared in executing a position control task. Integer-order PI controllers are not considered because it is expectable they give worst results, as shown in [9; 10]. The following specifications were considered (for both kind of motors): steady-state error $e_{ss} = 0$, $\omega_{gc} = 10$ rad/s, $PM = 45°$. A higher gain crossover frequency is not used because the step response of motor and robot link would be much faster, which is not desirable due to the robot-human interaction. Moreover, the chosen ω_{gc} is close to the crossover frequency (22.3 rad/s) of the uncompensated motor transfer function. Even with that frequency, a fast response of links will be obtained, then a pre-filter is necessary to decrease the response speed and the control signal magnitude.

The controllers have the parameters shown in Table 1. Note that both FOLaN and FOPI controllers are realized by rational transfer functions that approximate the irrational transfer functions. To this aim, a Padé approximation [3] or other techniques [21; 11; 12; 13; 14] can be used. For the FOLaN, a Padé approximation provided the following controller realization:

$$\begin{aligned}\overline{G}_{c1}(s) = 0.1693\,&\frac{(s+37.26)\,(s+5.671)}{(s+12.87)\,(s+2.792)}\times\\ &\times\frac{(s+1.435)\,(s+0.3107)}{(s+0.7053)\,(s+0.1076)}\,.\end{aligned} \tag{27}$$

For the FOPI controller, the realization was:

$$\overline{G}_{c2}(s) = 0.0343\,\frac{(s+693.9)\,(s+17.32)\,(s+1.019)}{s\,(s+94.72)\,(s+5.279)}\,, \tag{28}$$

where the integrator $\frac{1}{s}$ appears by putting $\frac{1}{s^{\nu}} = \frac{s^{1-\nu}}{s}$ in the controller, so that the operator $s^{1-\nu}$ is actually approximated. In this way, the controller allows to achieve a zero steady-state error if a step disturbance is applied.

Finally, note that a reference command filter was used to reduce overshoot:

$$G_f(s) = \frac{1}{1+0.5\, s}\,. \tag{29}$$

The time constant of the filter was adjusted by trial and error to obtain a reference step response without overshoot, which is important for various positioning tasks.

Simulation is performed by Simulink and results are illustrated below. The response to a reference step input and to a step disturbance applied at $t = 5$ s is shown in Fig. 4. The disturbance value was selected based on massive simulations of robot motion. The actual load disturbance varies with the robot configuration and depends on the torque that is due to the gravity force of the robot links and to the payload. The maximum value of disturbance during the transient operation is about 0.05 N m, and the mean value, which is used here, is much lower and around 0.02 N m.

The reference step response by the FOLaN network and the FOPI controller are approximately the same and achieve no overshoot. Note that overshoot is usually not desirable, then it is one of the primary design goals for robot position control, hence also in this paper. Namely, in case of overshoot, robot can hit and damage the manip-

Table 1. Controllers parameters settings.

Controller	Parameters			
FOLaN	$K_c = 6.6517$	$a = 0.0114$	$b = 21.7816$	$\alpha = 0.5032$
FOPI	$K_{p2} = 0.0343$	$T_{i2} = 0.0258$	$K_{i2} = 1.3279$	$\nu = 0.5$

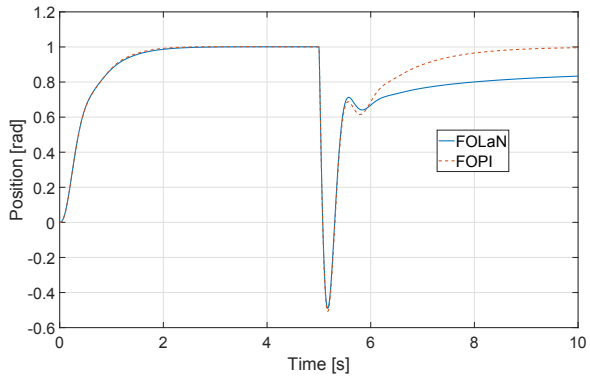

Fig. 4. Reference step response and disturbance rejection.

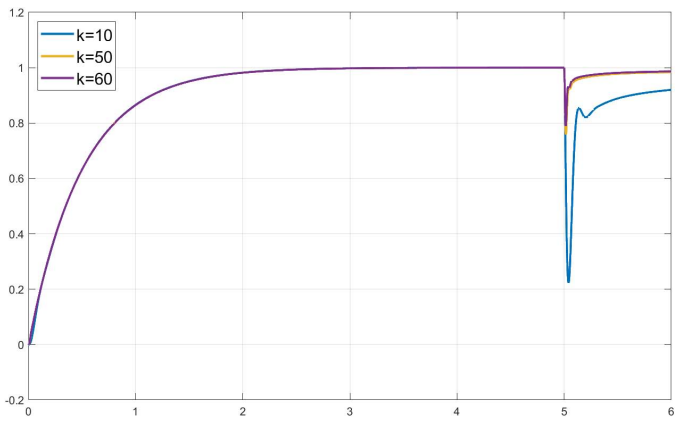

Fig. 5. Robustness to gain changes.

ulated object before it reaches the steady state, or it can be unsafe and dangerous in human-robot interaction. Moreover, because of the robustness of the fractional controllers, the no-overshoot response (or the iso-damping property) can be guaranteed with large variations in the process gain, which is an obvious and huge advantage over the classical PI controller. Namely, the FOLAN control system response was tested for different values of the process gain, which was increased 10, 50 and 60 times. The results are shown in Fig. 5. This benefit can be verified by the compensated Bode diagram, in which flatness of the phase curve around ω_{gc} (see Fig. 7) guarantees the obtained behavior for wide variations in the process gain.

Disturbance is properly rejected by the FOPI controller that includes an integrator to achieve a zero steady-state error, as previously shown. Instead, the FOLaN shows a static error. Namely, FOLaN is not primarily designed to reject disturbance signals. Instead, it is designed to achieve reference step response with no overshoot and with zero steady-state error, and more importantly, to maintain the iso-damping property even with large variations in the process gain (the same idea was presented in [23]). Future work will consider design of a fractional compensator with an integrator in its structure, so that disturbance signals are adequately rejected. Note that the static error becomes negligible if the gear ratio between the motor and robot is sufficiently high, hence the disturbance effect resulting from the robot and acting on the motor shaft becomes very small. Moreover, the undershoot is significant because a step disturbance is applied and the settling time is not optimized. These characteristics can be improved if

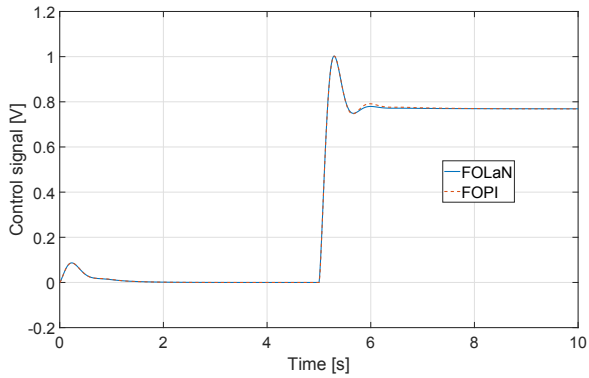

Fig. 6. Control signal.

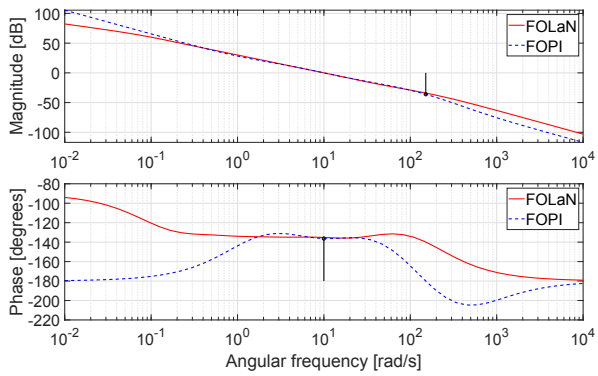

Fig. 7. Bode diagrams of the compensated system with a FOLaN and a FOPI controller.

disturbance is taken into account in the controller design. An explicit disturbance compensation can be made by considering a robot dynamic model that includes the mechanical coupling and by taking into account the robot position, velocity, and acceleration. However, this is not the aim of this paper and is matter of further work.

The control signal by the FOLaN and FOPI controllers is illustrated in Fig. 6. As it can be verified, the two signals, hence the related control efforts, are very similar. Moreover, the command signal shows no extreme peak values that can bring actuator to saturation. The maximum control input value for the DC motor is 32 V. However, the controller is not designed to be optimal from the control input value point of view. In practical implementation, an anti-windup scheme is used to ensure good response in case of control input saturation.

The frequency response characteristics are shown by the Bode diagrams in Fig. 7. The plots clearly indicate that the phase and magnitude specifications are met in the gain crossover frequency $\omega_{gc} = 10$ rad/s: magnitude is 1 and phase is about $-136°$ for a phase margin of $44°$. The FOLaN and FOPI controllers provide a flat phase diagram around ω_{gc}, so that the phase margin stays nearly constant if the process gain (and ω_{gc}) changes, which gives robustness to the loop with fractional compensators. Moreover, the FOPI controller shows a gain margin $GM \approx$ 36 dB in the phase crossover frequency of 150 rad/s.

5. CONCLUSION

This paper proposed the design of a FOLaN or a FOPI controller for motion control of three revolute joints of a robotic manipulator. Design of the FOLaN was by parameters optimization and based on the symmetrical optimum principle. Design of the FOPI was by a frequency-domain loop shaping technique. In both cases, specifications on the gain crossover frequency and phase margin were considered. The two controllers showed their effectiveness in obtaining the performance and robustness specifications. Flatness of the Bode phase diagram around the gain crossover is important and gives robustness to the loop with the FOLaN or the FOPI controller. Future work will perform experiments that were temporarily not possible.

ACKNOWLEDGEMENTS

This paper is based upon work from COST Action CA15225, a network supported by COST (European Cooperation in Science and Technology), and is also supported by the Serbia-Italy bilateral project "Advanced Robust Fractional Order Control of Dynamical Systems: New Methods for Design and Realization ADFOCMEDER".

REFERENCES

[1] H.-W. Bode. *Network Analysis and Feedback Amplifier Design*. Van Nostrand, New York, 1945.

[2] M. Č. Bosković, M. R. Rapaić, T. B. Šekara, V. Govedarica. Non-symmetrical optimum design method of fractional order PID controller. In *Proc. 2018 Int. Symp. on Ind. Electronics Conf. (INDEL)*. Banja Luka, Bosnia and Herzegovina, Nov. 1-3, 2018.

[3] M. Č. Bosković, M. R. Rapaić, T. B. Šekara, P. D. Mandić, M. P. Lazarević, B. Cvetković, B. Lutovac, M. Daković. On the rational representation of fractional order lead compensator using Padé approximation. In *Proc. 2018 7th Medit. Conf. on Embedded Computing*. Budva, Montenegro, June 10-14, 2018.

[4] M. Bucolo, A. Buscarino, L. Fortuna, M. Frasca. Forward action to make time-delay systems positive-real or negative-imaginary. *System & Control Letters*, 131, 2019.

[5] M. Bucolo, A. Buscarino, C. Famoso, L. Fortuna, M. Frasca. Control of imperfect dynamical systems. *Nonlinear Dynamics*, 98 (4), 2989–2999, 2019.

[6] V. Ćović, M. P. Lazarević. *Robot Mechanics*. Faculty of Mechanical Engineering, Belgrade, Serbia, 2009.

[7] H. Delavari, P. Lanusse, and J. Sabatier. Fractional order controller design for a flexible link manipulator robot. *Asian J. of Control*, 15 (3), 783–795, 2013.

[8] C. Kessler. Das symmetrische optimum. *Regelungstechnik*, 6, 395–400 and 432–436, 1958.

[9] P. Lino and G. Maione. Loop-shaping and easy tuning of fractional-order proportional integral controllers for position servo systems. *Asian J. of Control*, 15 (3), 796–805, 2013.

[10] P. Lino, G. Maione, S. Stasi, F. Padula, A. Visioli. Synthesis of fractional-order PI controllers and fractional-order filters for industrial electrical drives. *IEEE/CAA J. of Autom. Sinica*, 4 (1), 58–69, 2017.

[11] G. Maione. Continued fractions approximation of the impulse response of fractional order dynamic systems. *IET Contr. Theory & Appl.*, 2 (7), 564–572, 2008.

[12] G. Maione. Conditions for a class of rational approximants of fractional differentiators/integrators to enjoy the interlacing property. *IFAC Proceedings Volumes*, 44 (1), 13984–13989, 2011.

[13] G. Maione. Closed-form rational approximations of fractional, analog and digital differentiators/integrators. *IEEE J. Emerg. Sel. Topics in Circuits Syst.*, 3 (3), 322–329, 2013.

[14] G. Maione. Correction to "Closed-form rational approximations of fractional, analog and digital differentiators/integrators". *IEEE J. Emerg. Sel. Topics in Circuits Syst.*, 3 (4), 654, 2013.

[15] G. Maione. Multiple fractional networks for robust control design. In *Proc. 2017 Euro. Conf. on Circuit Theory and Design*. Catania, Italy, Sep. 4-6, 2017.

[16] G. Maione, P. Lino. New tuning rules for fractional PI^{α} controllers. *Nonlin. Dyn.*, 49 (1-2), 251–257, 2007.

[17] G. K. McMillan, Industrial applications of PID control. In R. Vilanova, A. Visioli, eds., *PID control in the third millenium*, 415–461. Springer, London, 2012.

[18] P. Melchior, Ch. Irnan, B. Metoui, A.Oustaloup. Robust path planning for mobile robot based on fractional attractive force in 3-dimension space. *IFAC Proceedings Volumes*, 45 (2), 577–582, 2012.

[19] C.A. Monje, Y.Q. Chen, B.M. Vinagre, D. Xue, V. Feliu. *Fractional-order Systems and Controls: Fundamentals and Applications*. Springer, London, 2010.

[20] A. Oustaloup. *La Commande CRONE. Command Robuste d'Ordre Non Entièr*. Ed. Hermès, Paris, 1991.

[21] A. Oustaloup, F. Levron, F. M. Nanot, B. Mathieu. Frequency band complex noninteger differentiator: characterization and synthesis. *IEEE Trans. Circuits Syst. I*, 47 (1), 25–39, 2000.

[22] A. Oustaloup, B. Mathieu, P. Lanusse. The CRONE control of resonant plants: application to a flexible transmission. *Europ. J. Control*, 1 (2), 113–121, 1995.

[23] A. Oustaloup, X. Moreau, M. Nouillant. The CRONE suspension. *Control Eng. Pract.*, 4 (8), 1101–1108, 1996.

[24] A. Oustaloup, B. Orsoni, P. Melchior, H. Linarès. Path planning by fractional differentiation. *Robotica*, 21 (1), 59–69, 2003.

[25] I. Podlubny. Fractional-order systems and $PI^{\lambda}D^{\mu}$-controllers. *IEEE Trans. Autom. Control*, 44 (1), 208–214, 1999.

[26] H. G. Sage, M. F. De Mathelin, E. Ostertag. Robust control of robot manipulators: A survey. *Inter. J. Control*, 76 (16), 1498–1522, 1999.

[27] T. B. Šekara. Modern methods of design, analysis, optimization and implementation of conventional control algorithms for processes with finite and infinite degrees of freedom. *Int. Journal of Electrical Engineering and Computing*, 1 (1), 11–20, 2017.

[28] T. B. Šekara, G. Vuković, B. Blanuša, M. R. Rapaić, B. Jakovljević. A novel method for optimization of PI/PID regulators based on symmetrical optimum method. In *Proc. Infoteh-Jahorina Conf.*, 804–807, 2015 (in Serbian).

[29] M. F. Silva, J. A. Tenreiro Machado, A. M. Lopes. Fractional order control of a hexapod robot. *Nonlinear Dynamics*, 38 (1-4), 417–433, 2004.